Integrating biological As(III) oxidation with Fe(0) electrocoagulation for arsenic removal from groundwater

Roy, Mrinal; van Genuchten, Case M.; Rietveld, Luuk; van Halem, Doris

DOI
10.1016/j.watres.2020.116531

Publication date
2021

Document Version
Final published version

Published in
Water Research

Citation (APA)
Roy, M., van Genuchten, C. M., Rietveld, L., & van Halem, D. (2021). Integrating biological As(III) oxidation with Fe(0) electrocoagulation for arsenic removal from groundwater. *Water Research*, *188*, 1-11. Article 116531. https://doi.org/10.1016/j.watres.2020.116531

Water Research 188 (2021) 116531

Contents lists available at ScienceDirect

Water Research

journal homepage: www.elsevier.com/locate/watres

Integrating biological As(III) oxidation with Fe(0) electrocoagulation for arsenic removal from groundwater

Mrinal Roy[a,*], Case M. van Genuchten[b], Luuk Rietveld[a], Doris van Halem[a]

[a] Water Management Department, Faculty of Civil engineering and Geosciences, Delft University of Technology, Stevinweg 1, 2628CN Delft, The Netherlands
[b] Department of Geochemistry, Geological Survey of Denmark and Greenland, Copenhagen DK-1350, Denmark

ARTICLE INFO

Article history:
Received 7 August 2020
Revised 13 October 2020
Accepted 16 October 2020
Available online 17 October 2020

Keywords:
Arsenic
Electrocoagulation
Drinking water
Iron
Groundwater

ABSTRACT

Arsenic (As) is a toxic element present in many (ground)water sources in the world. Most conventional As removal techniques require pre-oxidation of the neutral arsenite (As(III)) species to the negatively charged arsenate (As(V)) oxyanion to optimize As removal and minimize chemical use. In this work, a novel, continuous-flow As removal system was developed that combines biological As(III) oxidation by bacteria with Fe electrocoagulation (EC), an Fe(0)-based electrochemical technology that generates reactive Fe(III) precipitates to bind As. The bio-integrated FeEC system (bio-FeEC) showed effective oxidation and removal of 150 µg/L As(III), without the need of chemicals. To remove As to below the WHO guideline of 10 µg/L, 10 times lower charge dosage was required for the bio-FeEC system compared to conventional FeEC. This lower Fe dosage requirement reduced sludge production and energy consumption. The As(III) oxidizing biomass was found to consist of bacteria belonging to *Comamonadaceae, Rhodobacteraceae* and *Acidovorax*, which are capable of oxidizing As(III) and are common in drinking water biofilms. Characterization of the As-laden Fe solids by X-ray absorption spectroscopy indicated that both bio-FeEC and conventional FeEC produced solids consistent with a mixture of lepidocrocite and 2-line ferrihydrite. Arsenic bound to the solids was dominantly As(V), but a slightly higher fraction of As(V) was detected in the bio-FeEC solids compared to the conventional FeEC.

1. Introduction

Arsenic (As) contamination of drinking water sources, especially groundwater, has been a major global concern affecting many countries in the world, including Argentina, Bangladesh, Cambodia, China, India, Mexico, the United States and Vietnam. It has been estimated that around 94–220 million people worldwide have been exposed to groundwater with toxic As concentrations (Podgorski and Berg, 2020). In water sources, As is mainly present in two inorganic forms: arsenite (As(III)) and arsenate (As(V) (Wan et al., 2011), with the As(III) species being more toxic and more prevalent in reduced groundwater aquifers than As(V) (Katsoyiannis and Zouboulis, 2004; Nicomel et al., 2015). Chronic exposure to As in drinking water causes various diseases, such as skin, bladder and lung cancers, reproductive disorders and neurodevelopmental disease in children (Kapaj et al., 2006; Tseng, 1977). Hence, it is essential to remove As from contaminated water meant for drinking purposes, with the provisional drinking water guideline of 10 µg/L set by the World Health Organization (WHO) (WHO, 2004).

Many techniques have been proposed to remove As from drinking water, such as coagulation and flocculation, ion exchange, adsorption to activated alumina or iron based sorbents and reverse osmosis (Feenstra et al., 2007; Mondal et al., 2013). The efficiency of these techniques is improved by pre-oxidation of the neutral As(III) species to the negatively charged As(V) oxyanion ($H_2AsO_4^-$/$HAsO_4^{2-}$) (Goren et al., 2020; Kim and Nriagu, 2000), which is removed more readily by ion exchange, precipitation and adsorption (Kumar et al., 2004; Wan et al., 2011). Effective As(III) oxidation can be performed with chemical oxidants, including O_3, NaClO and $KMnO_4$ (Kim and Nriagu, 2000; Sorlini and Gialdini, 2010). However, chemical oxidants can be expensive and can generate unwanted by-products (Jackman and Hughes, 2010) that require additional treatment, which increases the cost and complexity of treatment (Katsoyiannis and Zouboulis, 2004). Hence,

* Corresponding author.
E-mail addresses: m.roy-1@tudelft.nl, mrinalroy1994@gmail.com (M. Roy).

https://doi.org/10.1016/j.watres.2020.116531

new methods are needed that can overcome the drawbacks of conventional chemical methods to oxidize and remove As(III).

The biological oxidation of As(III) by arsenic oxidizing bacteria (AsOB) is a promising alternative to chemical oxidation because AsOBs do not need auxiliary chemicals to oxidize As(III), which reduces the supply chain and costs of As removal (Kamei-Ishikawa et al., 2017). Native AsOBs have been detected in a wide range of conditions, including in As contaminated water and sediments (Ito et al., 2012), and are hypothesized to oxidize As(III) as a detoxification or energy generation (for growth) mechanism (Muller et al., 2003; Santini et al., 2000). Recently, biological oxidation of As(III) has also been reported in laboratory and industrial scale rapid sand filter systems, due to growth and accumulation of an AsOB community in filter beds, ripened with As(III) contaminated groundwater (Crognale et al., 2019; Gude et al., 2018; Lytle et al., 2007).

After biological As(III) oxidation, an additional treatment step is subsequently required to remove the dissolved As(V). One low-cost and chemical-free method is Fe(0) electrolysis, also known as Fe electrocoagulation (EC), which involves in-situ generation of Fe(III) precipitates to potentially bind As (Holt et al., 2005; Mollah et al., 2004; Moussa et al., 2017). In EC, a small electric current is applied to Fe(0) electrodes in contact with contaminated water to generate Fe(II) ions, which are then oxidized by dissolved oxygen (DO) to produce reactive Fe(III) precipitates with a high As sorption affinity (van Genuchten et al., 2012). After As sorption, the As-rich Fe(III) precipitates generated by EC can be removed by rapid sand filtration or gravitational settling. While FeEC can remove both As(III) and As(V) from water, the removal of As(III) requires substantially more Fe (proportional to charge passed) and treatment time than As(V) (Amrose et al., 2013; Wan et al., 2011). Therefore, pre-oxidizing As(III) should be considered to decrease the required energy and amount of produced sludge for equivalent As removal.

In this study, biological As(III) oxidation and FeEC were combined in a continuous flow setup. This type of bio-FeEC system, according to our knowledge, has not been demonstrated previously, but has the potential to substantially reduce Fe sludge production and energy consumption. We evaluated the As removal efficacy of bio-integrated FeEC and conventional FeEC in view of the biological conversion of dissolved As(III) and the molecular-scale structure and As uptake mechanism of the generated solid Fe(III) precipitates.

2. Materials and methods

2.1. Chemicals

Dutch non-chlorinated, tap water (characteristics in Table S1) was used as the model water for all experiments. Both As(III) and As(V) were added to the tap water from As(III) and As(V) stock solutions that were prepared by dissolving defined amounts of sodium (meta)arsenite ($NaAsO_2$) or sodium arsenate dibasic heptahydrate ($Na_2HAsO_4 \bullet 7H_2O$) (Sigma-Aldrich) to 18.2 mΩ.cm ultrapure water. The pH of the experimental solutions was adjusted with NaOH or H_2SO_4 (Merck Millipore) and the water conductivity was increased to 1200 ± 300 µS/cm by adding NaCl (Sigma-Aldrich).

2.2. Experimental setup

2.2.1. FeEC batch reactor

Batch EC experiments were conducted to understand the impact of charge dosage (CD), charge dosage rate (CDR) and initial As oxidation state on As removal, which informed our selection of operating parameters during the pilot-scale continuous flow experiments. The FeEC batch reactor consisted of a 1 L glass beaker containing 0.8 L As solution (tap water spiked with As(III) or As(V)) and two Fe electrodes (one cathode and one anode, Steel S235) in contact with the solution (Fig. 1(A)). The electrodes had dimensions of 50 mm x 20 mm x 0.5 mm, with a total submerged surface area of 12 cm^2 each and an inter-electrode gap of 1 cm. Before experiments, the electrodes were immersed in 0.01 M H_2SO_4 for 2 min and abraded with sand paper to remove any scale and rinsed with demineralized water. The electrodes were connected to a direct current (DC) power supply (TENMA® 72–10,500) to generate the Fe precipitates. The initial pH of the solution in all experiments was measured using a multimeter (WTW™ MultiLine™ Multi 3630 IDS) and was maintained between 7.0–8.0 by manual additions of 0.01 M H_2SO_4 and 0.1 M NaOH. In all EC batch experiments, the solutions were stirred using a magnetic stirrer (LABINCO L23) at 150 rpm. The initial DO was measured between 8.0–9.0 mg O_2/L using the multimeter.

In FeEC, the As removal efficiency depends on the amount of Fe generated in the solution and the rate at which it is generated Amrose et al., 2013). The amount and rate of Fe generated is proportional to the CD, (q in C/L) and CDR, (dq/dt in C/L/min) by Faraday's law (Eq. (1) and ((2)).

$$W = \frac{qM}{nF} = \frac{itM}{nFV} \quad (1)$$

$$\frac{dq}{dt} = \frac{i}{V} \quad (2)$$

where, W = amount of dissolved electrode material (mg/L); i = current (mA); t = electrolysis time (min); M = molecular weight of Fe (mg/mol) = 55,845; F = Faraday's constant (96,485 C/mol); n = number of transferred electrons (2 for Fe); V = solution volume (L).

The batch experiments were performed by applying a range of CD and CDRs to tap water containing 150 µg/L As(III) or As(V). Table 1 shows the applied CD and CDRs for the batch experiments along with the corresponding electrolysis time, applied current and the theoretical amount of Fe generated by Faraday's law. To determine As removal for a given CD, water samples were collected before and after EC (without additional mixing time or precipitate settling) and analyzed for total As and Fe, as well as aqueous As(III) and As(V).

2.2.2. Biological filter columns

Biological filter columns were used to establish an As(III) oxidizing microbial community in the filter beds, through ripening with As(III) water. The setup consisted of two duplicate down flow cylindrical columns (2 m high, 9 cm diameter, made from PVC) containing an anthracite layer (size fraction = 2.0 - 4.0 mm) coarse sand layer (size fraction = 1.4 – 2.0 mm) and garnet layer (size fraction = 0.3 - 0.6 mm), each 30 cm high (Fig. 1(B)). Before the experiments, the columns were backwashed with tap water until the supernatant was visually clear. The columns were then loaded continuously with tap water spiked with 150 µg/L As(III) for 49 days at a flow rate of 1 m/h to establish the oxidizing biomass. A supernatant level of 40 cm was maintained above the anthracite bed. The development of As(III) oxidation in the columns was monitored by measuring As speciation in the influent and effluent at 7 day intervals.

After ripening, column effluents from both columns were taken from the bottom location of the anthracite bed (As speciation showed >95% oxidation of 150 µg/L influent As(III) in the anthracite bed at 49 days) and FeEC was applied in batch mode. These separate experiments were performed to verify the performance of FeEC in solutions where As(III) was oxidized biologically and to determine the minimum CD (i.e. Fe dosage) required to remove 150 µg/L oxidized As(V) below 10 µg/L.

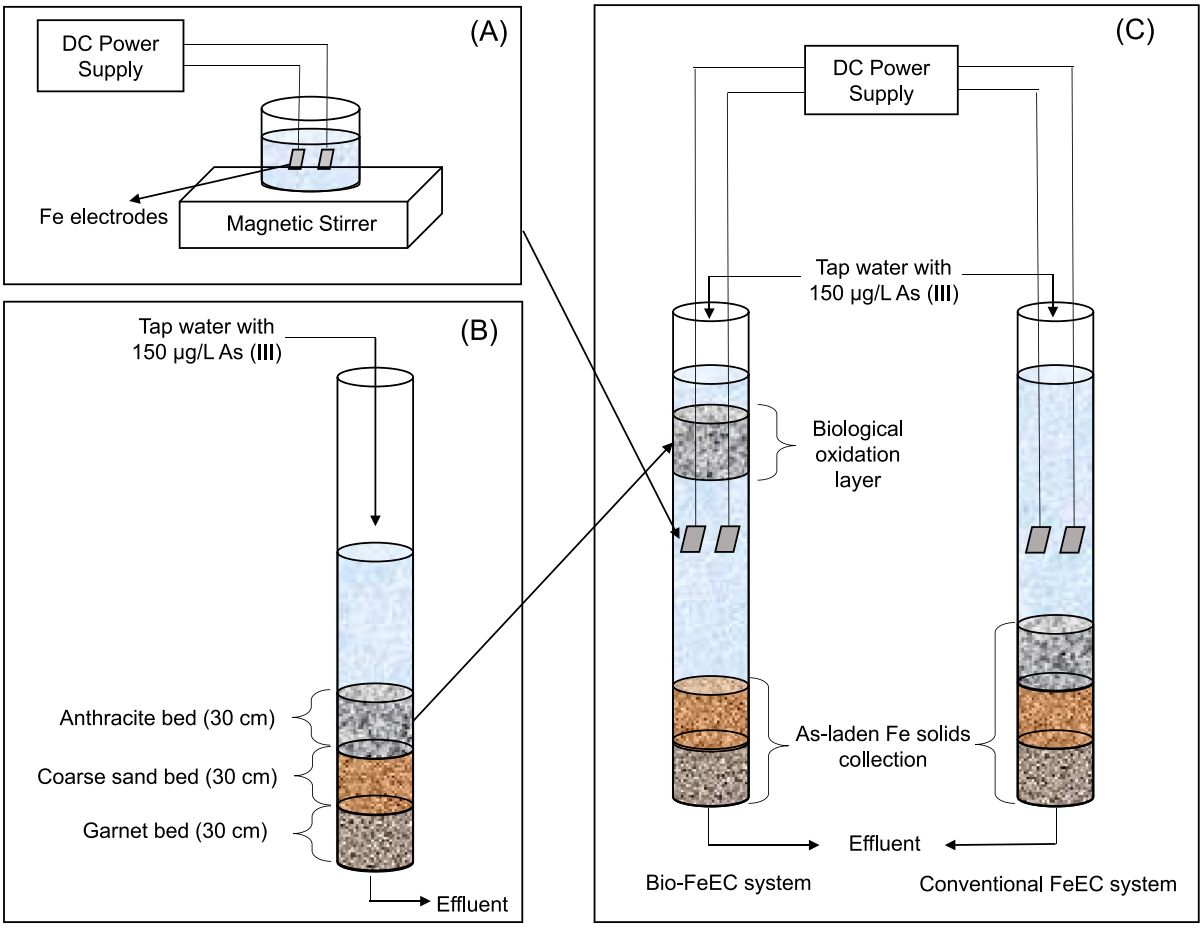

Fig. 1. Schematic diagram of the various experimental setups (A) batch FeEC experiments, (B) biological column experiment and (C) integrated bio-FeEC and conventional FeEC systems used during this study.

Table 1
List of operational parameters varied during FeEC batch experiments.

CD (C/L)	CDR (C/L/min)	EC Time (min)	Solution Volume (L)	Applied Current (Ampere)	Theoretical Fe conc. (mg/L)
10	5/15/60	2/0.67/0.17	0.8	0.07/0.2/0.8	2.90
25	5/15/60	5/1.67/0.42	0.8	0.07/0.2/0.8	7.26
50	5/15/60	10/3.33/0.83	0.8	0.07/0.2/0.8	14.51
100	5/15/60	20/6.67/1.67	0.8	0.07/0.2/0.8	29.02
150	5/15/60	30/10/2.50	0.8	0.07/0.2/0.8	43.53
200	5/15/60	40/13.33/3.33	0.8	0.07/0.2/0.8	58.04

2.2.3. Bio-FeEC system

After performing the FeEC batch experiments and establishing the As(III) oxidizing biomass, the integrated bio-FeEC set-up was assembled. The setup for the bio-FeEC system consisted of a similar down flow column as described in Section 2.2.2, augmented with an FeEC electrochemical cell. The column contained the ripened anthracite layer (containing oxidizing biomass) at the top followed by an FeEC cell, consisting of two Fe-electrodes (60 mm x 30 mm x 0.5 mm) connected to the DC power supply. The bottom of the column contained sand layers to collect the generated Fe solids during FeEC (Fig. 1(C)). An identical control FeEC flow-through system was created that consisted of only a conventional FeEC cell without a biological oxidation pre-layer (Fig. 1(C)). Tap water spiked with 150 µg/L As(III) was introduced to both systems at 1 m/h.

The bio-FeEC and conventional FeEC systems were run for 3 days, with an experimental run time of 6 h each day during which the FeEC cell was operated. After 6 h, the current applied to the FeEC cell was stopped and the As(III)-spiked tap water was allowed to flow through the columns continuously. After 3 days, the two systems were backwashed to collect the As-laden Fe solids that were trapped in the bottom sand layers for molecular-scale characterization by Fe and As K-edge X-ray absorption spectroscopy (XAS). For both column systems, the As removal efficiency was determined over the 6 h operating cycles by measuring the difference in dissolved As concentrations at the influent and just above the lower sand layers.

2.3. Chemical analyses

Water samples (in triplicates) were collected (1) unfiltered, (2) filtered over 0.45 µm polysthersulfone filters (Macherey-Nagel GmbH & Co. KG), and (3) filtered over 0.45 µm filters and an anionic resin (for As speciation). After collection, the samples were acidified using ultrapure nitric acid (ROTIPURAN® Ultra 69%) to dissolve any Fe precipitates. The samples were then stored at

4 °C before analysis for total As and Fe, as well as aqueous As(III) and As(V) by inductively coupled plasma mass spectrometry (ICP-MS, Analytikal Jena model PlasmaQuant MS). For As speciation, an anionic exchange resin (Amberlite* IRA-400 chlorite form resin) was used following the Clifford method as explained in Gude et al. (2018).

2.4. X-ray absorption spectroscopy

Solids for Fe and As K-edge XAS analysis were obtained by backwashing the bio-FeEC and conventional FeEC columns and filtering the backwashed water with filter papers. The filter papers containing the solids were then stored at −80 °C before preparation for XAS analysis. Fe and As K-edge XAS data were collected at beam line 2–2 of the Stanford Synchrotron Radiation Lightsource (SSRL, Menlo Park, USA). Fe K-edge XAS data were recorded at room temperature out to k of 13 $Å^{-1}$ and As K-edge XAS data were recorded at liquid nitrogen temperatures (≈80 °K) in fluorescence mode out to k of 14 $Å^{-1}$. Beam calibration was performed by setting the maximum of the first derivative of Fe(0) to 7112 eV or Au(0) to 11,919 eV for Fe and As K-edge XAS data, respectively. The SixPack software was used for spectral alignment, averaging and background subtraction (Webb, 2005), following standard procedures (van Genuchten et al., 2012). The EXAFS spectra were extracted using k^3-weighting and were Fourier-transformed using a Kaiser-Bessel window with dk of 3 $Å^{-1}$ over the k-range 2 to 11 $Å^{-1}$ for Fe data or 2 to 13 $Å^{-1}$ for As data.

The As K-edge XAS data were analyzed by linear combination fits (LCFs) of the XANES spectra and shell-by-shell fits of the EXAFS spectra using the SixPack software. The LCFs were performed over the energy range of 11,860 to 11,880 eV using reference spectra of As(III) and As(V) adsorbed to two line ferrihydrite (2LFh), which were collected previously at beam line 4–1 of SSRL under similar conditions as the current data set. The shell-by-shell fits were performed in $R + \Delta R$-space based on algorithms derived from IFEFFIT (Newville, 2001). Theoretical phase and amplitude functions for single and multiple scattering paths used in the fits were calculated using FEFF6 (Rehr et al., 1992) and were derived from the structure of scorodite (Kitahama et al., 1975). Additional details on XAS sample preparation and data collection and the shell-by-shell fitting procedure are provided in the Supplementary Materials.

2.5. Microbial characterization

To characterize the As(III) oxidizing biomass that grew and accumulated in the biological sand filters due to ripening with As(III)-rich water, a set of duplicate up-flow biological sand columns (1 m x 4 cm diameter, PVC) containing quartz filter sand (size fraction = 0.7–1.25 mm; bed height = 75 cm) was ripened with tap water containing 100 µg/L As(III) for a period of 60 days (Figure S1). After establishing the oxidizing biomass on the sand bed, sand samples (100 ml) were taken for DNA extraction at the bottom (15 cm) of the columns (location of influent) to characterize the biomass by high-throughput sequencing (HTS) of 16S rRNA genes.

Total genome DNA of the biomass on the sand samples was extracted using CTAB/SDS method. The concentration and purity of the DNA was monitored on 1% agarose gels and the DNA was diluted to 1 ng/μL using sterile water depending on the concentration. The bacterial 16S rRNA genes were amplified using specific primer and the PCR reactions were carried out with a Phusion® High-Fidelity PCR Master Mix (New England Biolabs). The PCR products were mixed with same volume of 1X loading buffer to operate electrophoresis on 2% agarose gel for detection. Samples with a bright main strip between 400 and 450 bp were considered for further analysis. The PCR products were then mixed in equidensity ratios and purified using Qiagen Gel Extraction Kit (Qiagen, Germany). NEBNex t® Ultra™ DNA Library Pre Kit (Illumina) was then used to generate sequencing libraries. The library quality was assessed on the Qubit@ 2.0 Fluorometer (Thermo Scientific) and Agilent Bioanalyzer 2100 system and sequenced on an Illumina platform to generate 250 bp paired-end reads. Paired-end reads were merged using FLASH (V1.2.7) (Magoč et al., 2011) to generate raw tags on which quality filtering was performed according to the QIIME(V1.7.0) (Caporaso et al., 2010) to generate high-quality clean tags. The tags were then compared with the reference Gold database using the UCHIME algorithm (Edgar et al., 2011) to obtain effective tags by detecting and removing chimera sequences.

Uparse software (Uparse v7.0.100) (Edgar, 2013) was used for sequence analysis and sequences with ≥ 97% similarity were assigned to the same Operational Taxonomic Units (OTUs). To obtain taxonomic information the representative sequence for each OTU was annotated by the RDP classifier (Version 2.2) (Wang et al., 2007) algorithm using GreenGene Database (Desantis et al., 2006).

3. Results and discussion

3.1. As removal in FeEC batch experiments

In order to understand the dependency of As(V) and As(III) removal on different EC operational parameters in the specific test water matrix, batch FeEC experiments were conducted. Fig. 2 shows the changes in dissolved As(III) and As(V) concentrations over the various applied CD values (0–200 C/L) at a CDR of 15 C/L/min. It was observed that as the CD increased, the dissolved As concentration decreased, which is consistent with previously reported EC batch studies (Amrose et al., 2013; Delaire et al., 2017; Goren et al., 2020; van Genuchten et al., 2012; Wan et al., 2011). The concentration of total Fe increased linearly with CD and matched the theoretical Fe concentration based on Faraday's law (Eq. (1)), (i.e. Faradaic efficiency = 1) (Müller et al., 2019). At CD values of 100 C/L and above (i.e. Fe dosages > 29 mg/L or Fe:As > 260 (mol:mol)), the dissolved As level decreased below the WHO guideline of 10 µg/L regardless the initial As oxidation state, and reached as low as ≤ 2 µg/L for CDs of 150 and 200 C/L. Since As removal in FeEC occurs via sorption to co-precipitated Fe(III) (oxyhydr)oxides (Kobya et al., 2016), the enhanced As removal at increasing CD can be explained by a higher concentration of Fe(III) precipitates and the corresponding availability of more As sorption sites.

Although both As(III) and As(V) removal was observed in FeEC batch experiments, solutions initially containing As(V) required a lower CD (10 C/L or Fe:As = 26 (mol:mol)) than As(III) (100 C/L or Fe:As = 260 (mol:mol)) to meet the WHO guideline of 10 µg/L. This result can be explained by the higher affinity of the generated Fe precipitates for As(V) than As(III) (Roberts et al., 2004).

With As(III) as the initial species, the oxidation to As(V) in solution was observed for CD values of 10, 25 and 50 C/L, which is consistent with the formation of reactive intermediates during FeEC operation that oxidize As(III) to As(V) (van Genuchten et al., 2012). At higher CD, dissolved As(V) was not observed, which can be explained by the presence of excess Fe leading to complete adsorption of dissolved As(V) (Dixit and Hering, 2003; Raven et al., 1998).

When CDR was varied, slightly more effective As(III) removal was observed at the lowest CDR of 5 C/L/min (Figure S2 and S3), consistent with previous work (Delaire et al., 2017; Li et al., 2012).

3.2. Biological As(III) oxidation in filter columns

The As speciation in the effluent of the duplicate down-flow biological filter columns over the experimental period of 49 days is

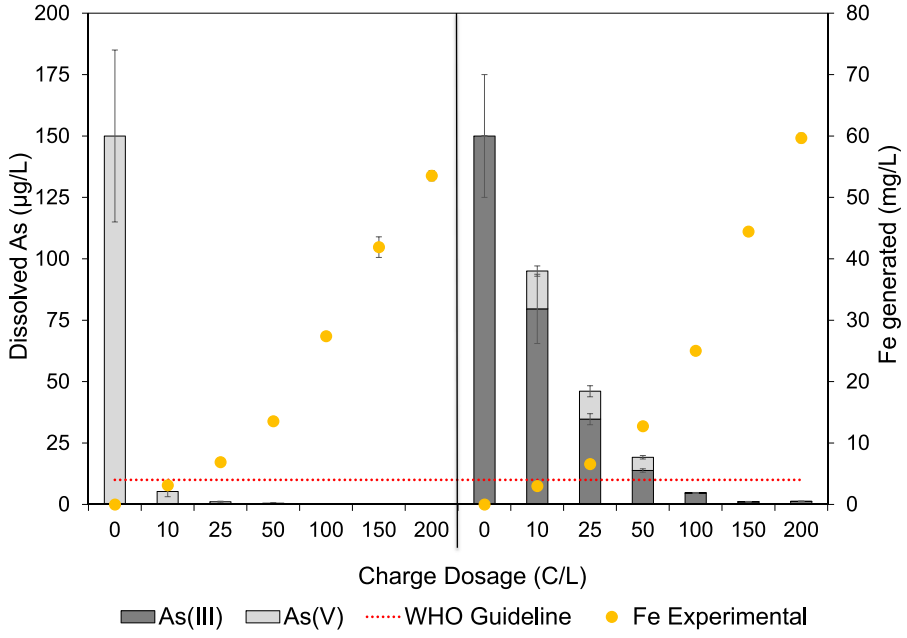

Fig. 2. Dissolved As concentration after FeEC in batch mode by applying various CD (0–200) C/L at 15 C/L/min CDR in tap water containing 150 µg/L As(V) (left) and As (III) (right) as initial As species.

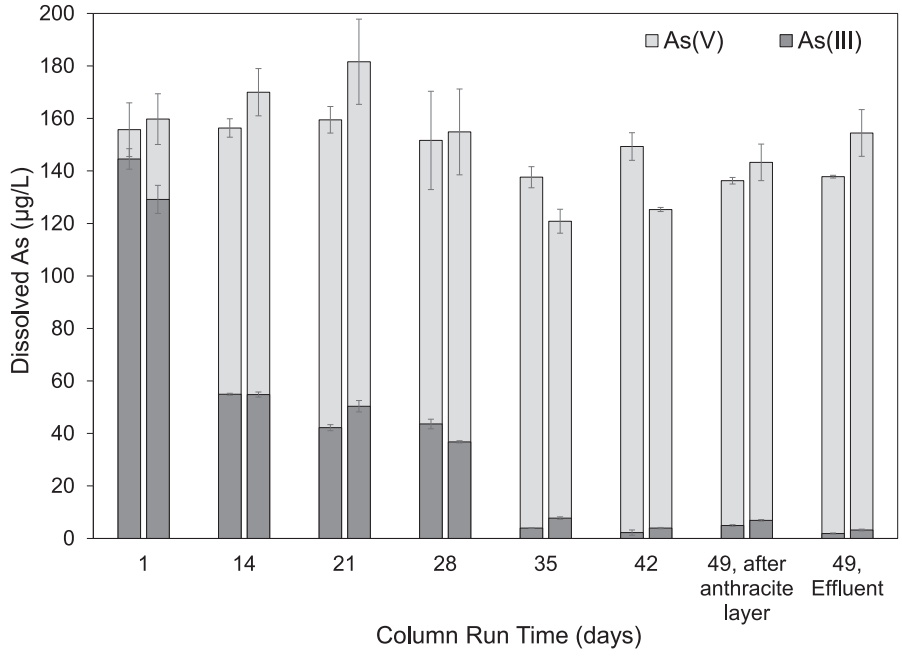

Fig. 3. As(III) and As(V) concentrations in the effluent of the duplicate biological filter columns during 49 days ripening with 150 ± 30 μg/L As(III) spiked tap water.

shown in Fig. 3. At the start of this ripening stage (day 1–28), 30 ± 10% of the influent As(III) was recovered in the filtrate. However, by 35 days, complete oxidation of 150 µg/L As(III) developed in the columns, which remained stable until the end of the experiment. The pH, DO, electrical conductivity and temperature were steady during the experimental period at 7.5 ± 0.5, 8 ± 1 mg/L, 300 ± 100 μS/cm and 20 ± 2 °C, respectively. Also, it must be noted that the total As concentration in the effluent was consistently lower (3–26%) than in influent, indicating adsorption to the fresh filter materials (anthracite, sand and garnet). On day 49, additional samples were collected for As speciation after the anthracite layer, revealing that >95% of As(III) was oxidized in the top layer. Therefore, this 30 cm layer was considered suitable for biological pre-treatment and was shifted upward prior to FeEC for follow-up experiments.

A similar As(III) oxidation pattern was observed in the two upflow columns, which were used for characterization of the accumulated As(III) oxidizing biomass (Figure S4). High-throughput sequencing (HTS) of the biomass DNA generated OTUs of 730 and 811, and 609 and 562 from duplicate samples of each column, respectively. Fig. 4(A) depicts the relative abundance (RA) (percentage of total OTUs) of the top 10 classes, which accounted for more than 97% of the entire biomass in each sample. *Alphaproteobacteria* and *Betaproteobacteria* were the two most abundant classes

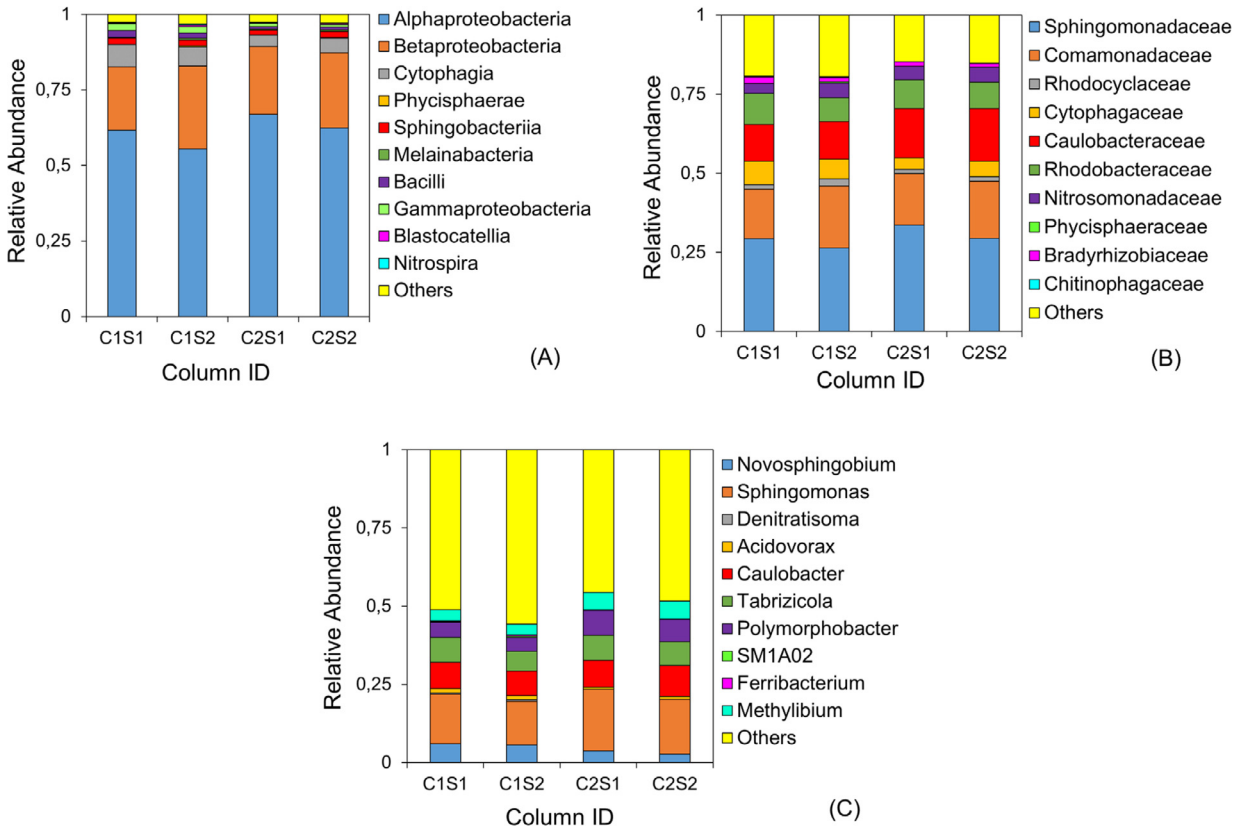

Fig. 4. Relative abundance (% of total OTUs) of the predominant bacterial communities in the accumulated As(III) oxidizing biomass of the duplicate up-flow biological columns at class (A), family (B) and genus (C) level. (C1, C2 = 2 columns; S1, S2 = duplicate sand samples from each column).

in the two columns having a RA of 55–67% and 21–28%, respectively, which is in agreement with findings of Cavalca et al. (2013). Both of these classes belong to the most abundant phylum *Proteobacteria* (Figure S5). Furthermore, classification at the family level showed the presence of microorganisms affiliated with *Comamonadaceae* (RA: 15–20%; Class: *Betaproteobacteria*) and *Rhodobacteraceae* (RA: 7.5–10%; Class: *Alphaproteobacteria*) (Fig. 4(B)), which are known to oxidize As(III) (Crognale et al., 2019). Additionally, the As(III) oxidizing genus *Acidovorax* (RA: 0.6–1.4%) in the *Comamonadaceae* family was also observed (Fig. 4(C)), which is a genus that is common in the rapid sand filters of drinking water treatment plants treating As free water (Vandermaesen et al., 2017), but that also oxidize As(III) (Cavalca et al., 2013). While As(III) oxidizing biomass is commonly reported in sand filters for groundwater treatment (Crognale et al., 2019; Gude et al., 2018; Katsoyiannis and Zouboulis, 2004), our results indicate that a similar As(III) oxidizing biomass can also develop in sand filters running on chlorine-free tap water, sourced from a surface water body.

3.3. As(III) removal by bio-FeEC

3.3.1. Batch experiments

After ripening of the biological columns, batch FeEC experiments were performed on the column effluent, which contained 150 µg/L As(V), to determine the optimal operational parameters for the continuous flow experiments. Fig. 5 shows the change in dissolved As(III) and As(V) concentrations after applying various CDs (0–200 C/L) at a CDR of 5 C/L/min to the column effluent and to an unoxidized As(III)-spiked tap water solution for reference. The As removal in the column effluent was similar to that of the FeEC experiment using tap water containing As(V) as the initial As species (Figure S2 (left)). For FeEC experiments in both the biological column effluent and the As(V) solution, a CD of 10 C/L (at CDR of 5 C/L/min) was able to remove 150 μg/L As to below the 10 μg/L WHO guideline, whereas a CD of 100 C/L was needed to achieve the same level with the reference As(III) solution.

The Faradaic efficiency for the FeEC experiments in the column effluents containing oxidized As(V) was near 1, which was similar to the values obtained for FeEC experiments in standard As(V) solution (Figure S2 (left)). This result suggests that biological As(III) oxidation did not impact the electrochemical oxidation of Fe(0) and the release of Fe(II) to the bulk solution.

3.3.2. Continuous flow experiments

The operating parameters of CD = 10 C/L applied at CDR = 5 C/L/min were selected for the continuous flow bio-FeEC experiments based on the results from the batch EC experiments using the biological column effluent. The voltage observed in the DC current supplier to achieve the required CD and CDR in both column systems was 2.1 V. Fig. 6 depicts the results during the 3 day experimental duration for both the bio-FeEC (left) and the conventional FeEC (right) continuous flow systems. The results indicate that both systems removed As, but only the bio-FeEC system was able to decrease As levels to below the WHO guideline of 10 μg/L, despite identical operating parameters (i.e. flow rate, CD, CDR). In the bio-FeEC system, the dissolved As concentration decreased from 150 ± 30 μg/L to approximately 2 ± 1 μg/L (98% removal). The dissolved As concentration was consistently higher than the WHO guideline in the conventional FeEC system, with approximately 38 ± 4 μg/L remaining in solution (73% removal), which consisted of 75 ± 5% As(III).

It was also observed that the As(III) removal efficiency of the conventional FeEC column was higher (73% As removal) than the FeEC batch experiments using the As(III)-spiked tap water (42% As

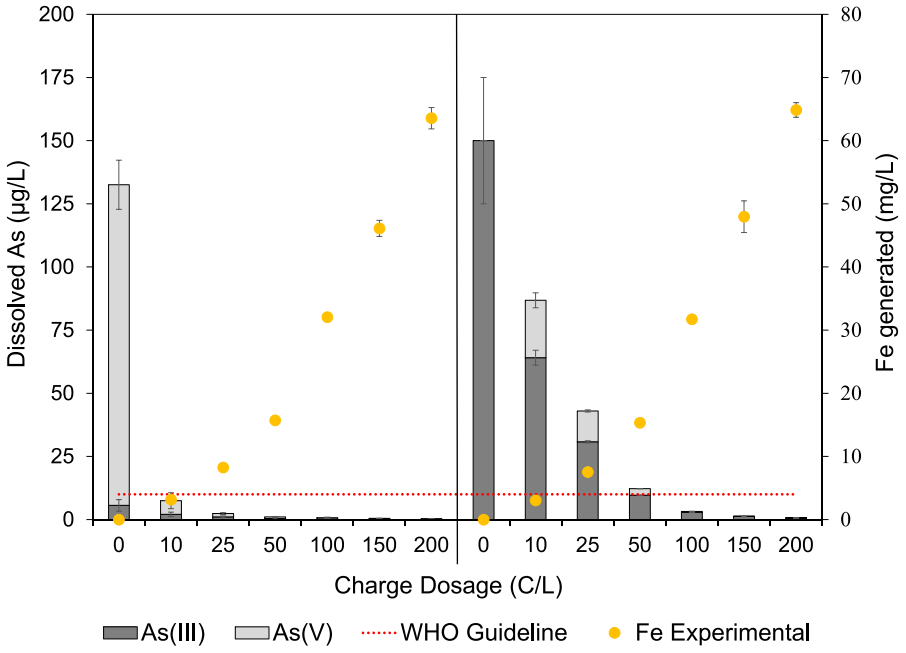

Fig. 5. Batch mode bio-FeEC (left) and conventional FeEC (right) treatment of 150 µg/L As(III) as a function of CD applied at 5 C/L/min CDR. The bio-FeEC experiments were conducted with the effluent of the biological anthracite layer; the conventional FeEC experiments are shown again in Figure S2 (right).

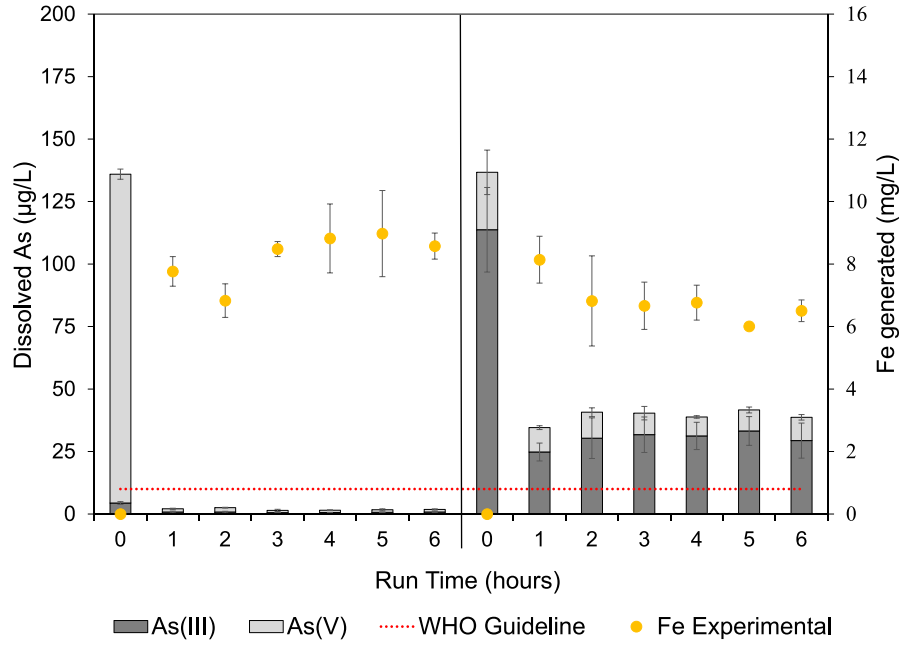

Fig. 6. Average As(III) removal during continuous flow mode bio-FeEC (left) and conventional FeEC (right) during 6 h experimental run time (executed in triplicate). FeEC was operated under 10 C/L CD at 5 C/L/min CDR.

removal), despite the similar operating parameters (CD = 10 C/L and CDR = 5 C/L/min). This result can be explained by the accumulation of Fe solids on top of the supporting filter layers in the continuous flow system. This explanation is based on the measured total Fe concentration of approximately 7 mg/L in unfiltered samples of the conventional FeEC column system, which is greater than the theoretical Fe value of 3 mg/L (Eq. (1)) expected based on Faraday's law. The accumulated Fe solids allow for extended contact time with dissolved As, resulting in greater As adsorption per Fe mass. Although the Fe concentration was also significantly higher than the theoretical Faradaic value in the bio-FeEC column, no difference in As removal per charge passed was observed in the bio-FeEC because of the nearly complete removal of the oxidized As(V). However, the accumulation of Fe in both continuous flow systems suggests that the bio-FeEC column could be operated at even lower CD and still achieve As(III) removal to below 10 μg/L.

3.4. Characterization of Fe-As solids

After the 6 h operating cycles over the 3-day experimental duration, the filter columns were backwashed and the solids were characterized by Fe and As K-edge XAS (Fig. 7). The Fe K-edge EX-

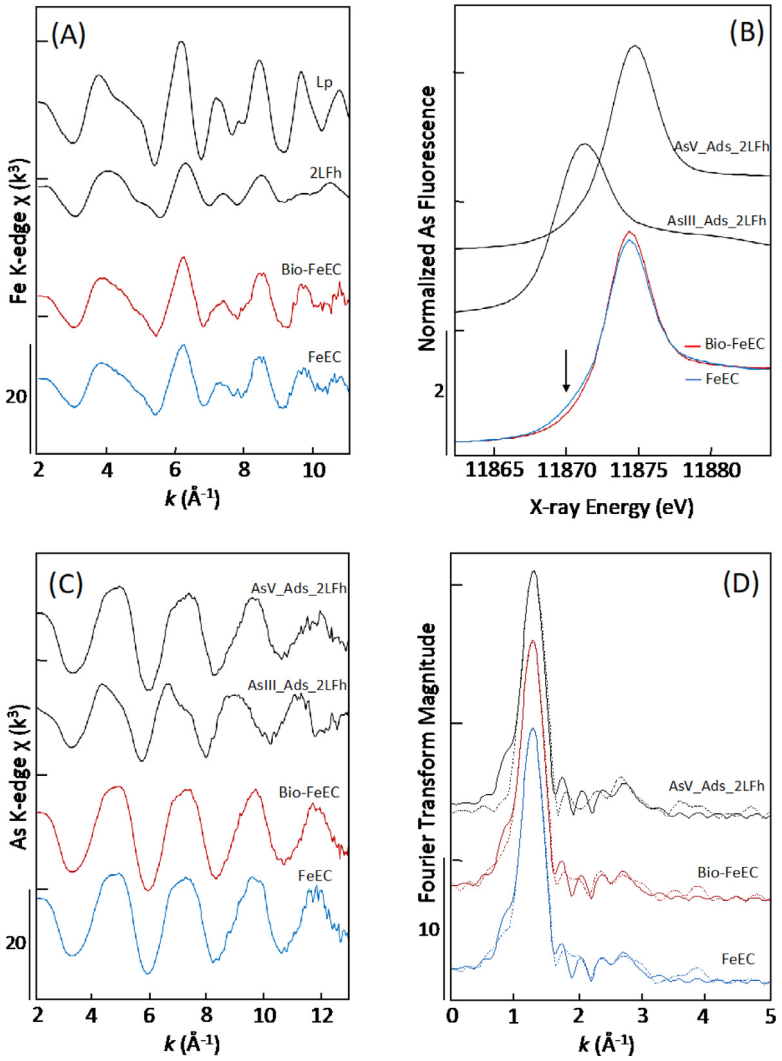

Fig. 7. (A) Fe K-edge EXAFS spectra of the solids produced in the bio-FeEC and conventional FeEC columns plotted below reference spectra of lepidocrocite (Lp) and 2-line ferrihydrite (2LFh). (B) As K-edge XANES spectra of the solids produced in the bio-FeEC and conventional FeEC columns plotted below reference spectra of As(III) and As(V) adsorbed to 2LFh. The arrow in B highlights a small shoulder indicative of As(III). (C) As K-edge EXAFS spectra of samples compared to the reference spectra of As(III) and As(V) adsorbed to 2-line ferrihydrite (2LFh). (D) Fourier-transformed As K-edge EXAFS spectra (data in dotted lines) and output of the shell-by-shell fits (model output in solid lines).

AFS spectra showed no notable difference in line shape or phase of the oscillations for samples collected from the bio-FeEC and conventional FeEC columns, indicating a similar average structure of the generated Fe(III) precipitates. Based on characteristic fingerprints in the EXAFS spectra, including the asymmetric first oscillation from 3 to 5.5 $Å^{-1}$, the solids are consistent with a mixture of lepidocrocite (γ-FeOOH) and poorly-ordered Fe(III) precipitates (e.g. 2-line ferrihydrite, 2LFh) (Fig. 7(A)). The formation of a mixture of lepidocrocite and 2LFh can be attributed to the composition of the As(III)-rich tap water (Table S1) and is consistent with solids formed in previous FeEC studies at similar pH and total As/Fe ratios (van Genuchten et al., 2014; Wan et al., 2011). Previous studies on Fe oxidizing bacteria have shown that Fe(III) precipitates produced by various types of bacteria often have unique structures because biogenic dissolved organic compounds can interfere with Fe(III) (oxyhydr)oxide crystallization pathway (Toner et al., 2009). However, the Fe K-edge EXAFS spectra of solids from both systems were similar, indicating that the bacteria upstream of the FeEC cell did not interfere with Fe(III) polymerization. Instead, the inorganic composition of the solution played a more important role in determining the Fe(III) precipitate structure. The formation of poorly-ordered solids, such as 2LFh, in the bio-FeEC and conventional FeEC system can be advantageous for As adsorption because of their higher proportion of reactive surface area per mass (i.e. specific surface area) compared to more crystalline Fe phases (Dixit and Hering, 2003).

The As K-edge XANES data for samples collected from the bio-FeEC and conventional FeEC systems indicate that the oxidation state of As bound to the solids was predominantly As(V) for both systems based on the position of the absorption maximum near 11,875 eV (Fig. 7(B) and (C)). The predominance of solid-phase As(V) in the conventional FeEC system is in line with the oxidation of As(III) during FeEC due to the formation of reactive intermediates (Li et al., 2012; van Genuchten et al., 2012). Although As(V) was the major species inbound to both bio-FeEC and conventional FeEC solids, the LCFs of the XANES spectra indicated a slightly higher As(III) percentage for solids in the conventional FeEC system (8%) compared to those of the bio-FeEC system (2%). These results confirm that the As removal pathway for both columns involved As(III) oxidation. However, unlike the bio-FeEC system, the abiotic As(III) oxidation pathway of the conventional FeEC column was not sufficient to oxidize all As(III). Consequently, As(III) was

observed bound to the Fe solids of the conventional FeEC column and was the dominant form of As in effluent, which was substantially higher (38 ± 4 μg/L) than the bio-FeEC system (2 ± 1 μg/L).

The As K-edge EXAFS spectra of the solids collected from both continuous flow systems were similar, consistent with the As K-edge XANES data, and both matched the reference spectrum of As(V) adsorbed to 2LFh. To confirm the exact As bonding mode to the Fe(III) precipitates in both systems, shell-by-shell fits of the Fourier-transformed EXAFS spectra were performed. The output of the fits is overlain to the data in Fig. 7(D) and the fitting parameters are summarized in Table S2. The fitting results were identical for both conventional FeEC and bio-FeEC samples within fit-derived standard errors, indicating a similar As uptake mode. The fitting output for both samples also matched that of the reference spectrum of As(V) adsorbed 2LFh. The first shell fits of the samples returned values for the As-O coordination number ($CN_{As\text{-}O}$) of 4.3 to 4.6 and As-O interatomic distance ($R_{As\text{-}O}$) of 1.69 Å which is consistent with tetrahedrally-coordinated As(V) (Waychunas et al., 1993). The second shell fits of both samples yielded $CN_{As\text{-}Fe}$ values of 1.4 to 1.6 and an $R_{As\text{-}Fe}$ of 3.28 Å, which was identical to the fits of As(V) adsorbed to 2LFh, within fit-derived standard errors (Table S2). Based on these fit-derived parameters, we conclude that As was taken up by the solids produced in both bio-FeEC and conventional FeEC systems via the binuclear corner-sharing (^{2}C) surface complex, where As(V) tetrahedra bind to the apical oxygen atoms of two adjacent edge-sharing FeO_6 octahedra (van Genuchten et al., 2012; Waychunas et al., 1993). We noted that the XANES LCFs revealed a slightly larger fraction of As(III) in the conventional FeEC sample that was not reflected in the shell-by-shell fitting results, which can be explained by the higher sensitivity of XANES analysis to small changes in As oxidation state. Therefore, the conclusions obtained with shell-by-shell fits of the EXAFS data did not account for the additional complexity of the FeEC solids, which contained 8% sorbed As(III).

3.5. Benefits and challenges of bio-FeEC

Our results indicate that integrating biological As(III) oxidation with FeEC can be advantageous to treat As(III) contaminated water because of the lower Fe dosage or CD requirement to achieve sufficiently low As levels in the effluent. At a CD value of 10 C/L, the bio-FeEC column removed As(III) to well below 10 μg/L, whereas As in the effluent of the conventional FeEC column was considerably greater than the WHO recommended limit. Based on the results of the batch experiments, the conventional FeEC column could have eventually achieved As removal to below 10 μg/L, but a much higher CD would be needed. This higher CD for equivalent As removal requires a substantially higher applied current or electrolysis time, which would lead to greater electricity consumption and a larger amount of Fe sludge generated. For instance in the bio-FeEC column, the average energy consumption and sludge production to remove 150 µg/L As(III) below 10 µg/L for a CD of 10 C/L under a constant voltage (U) of 2.1 V was 0.006 kWh/m^3 (by Eq. (3)) and 0.007 kg/m^3 respectively. Similarly for the conventional FeEC column to remove 150 µg/L As(III) below 10 µg/L a CD of 100 C/L might be necessary (as observed in the batch FeEC system, (Fig. 2)), which is 10 times higher than bio-FeEC, resulting in a tenfold increase in energy consumption and sludge generation of 0.06 kWh/m^3 (by Eq. (3)) and 0.07 kg/m^3 respectively. Compared to other removal techniques, the power required for treating the As-contaminated water by bio-FeEC (0.06 kWh/m^3) is nearly two orders of magnitude lower than the power requirement (3–4 kWh/m^3) reported for As treatment by membrane techniques (Schmidt et al., 2016). Furthermore, because Fe(III) precipitates form in the presence of As during FeEC, the amount of reactive surface area available for As sorption per mass of solid (50 µg As/mg Fe) is significantly higher than for other Fe-based strategies, including adsorption to pre-synthesized Fe(III) oxide adsorbents or Fe oxide coated sand filters (Thirunavukkarasu et al., 2003). Therefore, the amount of sludge generated by bio-FeEC for a given electrolyte composition is lower than other methods. However, it is important to note that direct comparisons of the power requirement and sludge production of different techniques is difficult because these parameters are highly dependent on solution composition. Hence, the values of power consumption and sludge generation obtained for the bio-FeEC system are relevant to the solution conditions used in this study and might not reflect exactly the values obtained in other types of As-contaminated water.

$$C_{energy} = Uq \quad (3)$$

where C_{energy} = Consumption of electricity per m^3 of water treated (Wh/m^3); U = Total cell potential (V); q = Charge dosage (C/L)

The advantage of pre-oxidizing As(III) in FeEC in terms of lower CD and Fe required for complete removal has been reported previously in systems where As(III) was oxidized by chemical or electrochemical methods (Flores et al., 2013; Zhang et al., 2014). However, in the bio-FeEC system, the oxidation is performed biologically without the need of chemicals or electricity, which is a benefit because chemicals can create secondary by-products in water (disinfection by-products for NaClO; (Jackman and Hughes, 2010)) and more electricity would lead to higher energy consumption. Furthermore, a separate chemical oxidation step can lead to more complex supply chains for As treatment, which is a major barrier to sustained operation of technologies, particularly in decentralized areas. Finally, the lower Fe sludge production in the bio-FeEC system compared to conventional FeEC also requires less waste management (i.e. landfill disposal) and reduces the backwashing frequency of the post filtration step due to less clogging of the filter beds. Although the bio-FeEC system produces less As-rich Fe sludge than conventional FeEC, proper handling and disposal of the sludge is still important from the perspective of safety and circularity. Identifying the most appropriate sludge disposal method is beyond the scope of our study, but one method could be to dewater the sludge by passive settling and subsequent drying for re-use in industry (e.g., brick production) (Hassan et al., 2014; Sullivan et al., 2010). Another approach can be stabilizing the sludge in concrete for re-use in local construction (Roy et al., 2019). However, in both cases, the toxicity characteristic leaching procedure (TCLP) test must be performed first to identify the leaching behavior of the waste, which ensures minimal environmental contamination (Sullivan et al., 2010).

Although our work suggests that the bio-FeEC system can be an effective alternative to conventional FeEC or other standard As removal techniques, some potential challenges of the system must be investigated before implementing it in practice. For example, whereas the biological layer can oxidize ammonium (NH_4^+) in groundwater (Gude et al., 2018), which is an added benefit, the biological layer can also enhance Fe(II) and manganese (Mn(II)) oxidation (Gülay et al., 2018; Vandenabeele et al., 1992). The oxidation of Fe(II) and Mn(II) in the biological layer can result in their removal due to deposition of the solid oxidation products in the layer, but this can also be disadvantageous as the deposited solids can clog the layer, requiring more frequent backwashing or a conventional aeration-filtration step prior to bio-FeEC. Furthermore, the presence of high concentrations of natural organic matter (NOM) and total organic carbon (TOC) in groundwater can impact the speciation of aqueous Fe(II) by complexation (Sundman, 2014), which alters Fe(II) oxidation kinetics, can decrease As adsorption on Fe solids by competing for sorption sites (Redman et al., 2002), and can enhance growth of the biological layer (Kott et al., 1997), which can potentially lead to increased amounts of organic matter in subsequent treatment stages due to washout of biologi-

cal material. However, we note that FeEC is effective at removing organic matter, which suggests that washout from the biological layer might not substantially decrease the quality of treated water (McBeath et al., 2020). The bio-FeEC system also requires a startup period to establish the AsOB-containing biofilm on the sand bed, which can lead to additional energy needed for continuous water pumping during ripening. This disadvantage can be avoided through accelerating the ripening phase by inoculating with already ripened sand from an existing As(III) treatment plant or by adding more Fe via FeEC to achieve sufficient As removal at the onset of treatment. Overall, the attractiveness of the bio-FeEC system lies particularly in that it can be implemented using locally available materials in conventional or decentralized systems (with electricity consumption offset by solar panels) which is appropriate for rural areas of South Asia, where As contamination of drinking water sources has led to catastrophic health impacts (Chakraborti et al., 2010).

4. Conclusions

In this study, the novel integrated system of biological As(III) oxidation and Fe electrocoagulation to treat As(III)-contaminated water was investigated. Compared to the abiotic, conventional FeEC system, the integrated biological FeEC system showed more effective oxidation and removal of 150 µg/L As(III) to below 10 µg/L without the need of chemicals. The bio-FeEC system reduced the Fe dosage required (by 10 times) compared to conventional FeEC. Hence, we propose that this integrated biological and electrochemical system can be a sustainable approach to remove As(III) from water, particularly in areas where costly and complex supply chains inhibit sustained operation of treatment methods..

Declaration of Competing Interest

The authors declare that they have no known competing financial interests or personal relationships that could have appeared to influence the work reported in this paper.

Acknowledgements

This project is supported by the Global Drinking Water program, TU Delft focusing on removal of health-based contaminants from water. The authors want to thank David de Ridder and Marjet Oosterkamp for their help while performing microbial community characterization. We thank Ryan Davis, Matthew Lattimer and Erik Nelson at SSRL for assistance during XAS data collection. Use of SSRL, SLAC National Accelerator Laboratory, was supported by the U.S. Department of Energy, Office of Science, Basic Energy Sciences, under Contract No. DE-AC02–76SF00515.

Supplementary materials

Supplementary material associated with this article can be found, in the online version, at doi:10.1016/j.watres.2020.116531.

References

Amrose, S., Gadgil, A., Srinivasan, V., Kowolik, K., Muller, M., Huang, J., Kostecki, R., 2013. Arsenic removal from groundwater using iron electrocoagulation: effect of charge dosage rate. J. Environ. Sci. Health - Part A Toxic/Hazardous Subst. Environ. Eng. 48 (9), 1019–1030. doi:10.1080/10934529.2013.773215.

Caporaso, J.G., Kuczynski, J., Stombaugh, J., Bittinger, K., Bushman, F.D., Costello, E.K., Fierer, N., Gonzalez Peña, A., Goodrich, J.K., Gordon, J.I., Huttley, G.A., Kelley, S.T., Knights, D., Koenig, J.E., Ley, R.E., Lozupone, C.A., Mcdonald, D., Muegge, B.D., Pirrung, M., … Knight, R., 2010. QIIME allows analysis of high-throughput community sequencing data. Nat. Methods 7 (5), 335–336. doi:10.1038/nmeth.f.303.

Cavalca, L., Corsini, A., Zaccheo, P., Andreoni, V., Muyzer, G., 2013. Microbial transformations of arsenic: perspectives for biological removal of arsenic from water. Future Microbiol. 8 (6), 753–768. doi:10.2217/fmb.13.38.

Chakraborti, D., Rahman, M.M., Das, B., Murrill, M., Dey, S., Chandra Mukherjee, S., Dhar, R.K., Biswas, B.K., Chowdhury, U.K., Roy, S., Sorif, S., Selim, M., Rahman, M., Quamruzzaman, Q., 2010. Status of groundwater arsenic contamination in Bangladesh: a 14-year study report. Water Res. 44 (19), 5789–5802. doi:10.1016/j.watres.2010.06.051.

Crognale, S., Casentini, B., Amalfitano, S., Fazi, S., Petruccioli, M., Rossetti, S., 2019. Biological As(III) oxidation in biofilters by using native groundwater microorganisms. Sci. Total Environ. 651, 93–102. doi:10.1016/j.scitotenv.2018.09.176.

Delaire, C., Amrose, S., Zhang, M., Hake, J., Gadgil, A., 2017. How do operating conditions affect As(III) removal by iron electrocoagulation. Water Res. 112, 185–194. doi:10.1016/j.watres.2017.01.030.

Desantis, T.Z., Hugenholtz, P., Larsen, N., Rojas, M., Brodie, E.L., Keller, K., Huber, T., Dalevi, D., Hu, P., Andersen, G.L., 2006. Greengenes, a chimera-checked 16S rRNA gene database and workbench compatible with ARB. Appl. Environ. Microbiol. 72 (7), 5069–5072. doi:10.1128/AEM.03006-05.

Dixit, S., Hering, J.G., 2003. Comparison of arsenic(V) and arsenic(III) sorption onto iron oxide minerals: implications for arsenic mobility. Environ. Sci. Technol. 37 (18), 4182–4189. doi:10.1021/es030309t.

Edgar, R.C., 2013. UPARSE: highly accurate OTU sequences from microbial amplicon reads. Nat. Methods 10 (10), 996–998. doi:10.1038/nmeth.2604.

Edgar, R.C., Haas, B.J., Clemente, J.C., Quince, C., Knight, R., 2011. UCHIME Improv. Sensit. Speed Chimera Detect. 27 (16), 2194–2200. doi:10.1093/bioinformatics/btr381.

Feenstra, L., Van Erkel, J., & Utrecht, L.V. (2007). Arsen. Groundw..

Flores, O.J., Nava, J.L., Carreño, G., Elorza, E., Martínez, F., 2013. Arsenic removal from groundwater by electrocoagulation in a pre-pilot-scale continuous filter press reactor. Chem. Eng. Sci. 97, 1–6. doi:10.1016/j.ces.2013.04.029.

Goren, A.Y., Kobya, M., Oncel, M.S., 2020. Arsenite removal from groundwater by aerated electrocoagulation reactor with Al ball electrodes: human health risk assessment. Chemosphere 251, 126363. doi:10.1016/j.chemosphere.2020.126363.

Gude, J.C.J., Rietveld, L.C., van Halem, D., 2018. Biological As(III) oxidation in rapid sand filters. J. Water Process Eng. 21, 107–115. doi:10.1016/j.jwpe.2017.12.003.

Gülay, A., Çekiç, Y., Musovic, S., Albrechtsen, H.-J., Smets, B.F., 2018. Diversity of Iron oxidizers in groundwater-fed rapid sand filters: evidence of Fe(II)-dependent growth by curvibacter and undibacterium spp. Front. Microbiol. 9. doi:10.3389/fmicb.2018.02808.

Hassan, K.M., Fukushi, K., Turikuzzaman, K., Moniruzzaman, S.M., 2014. Effects of using arsenic-iron sludge wastes in brick making. Waste Manage. (Oxford) 34 (6), 1072–1078. doi:10.1016/j.wasman.2013.09.022.

Holt, P.K., Barton, G.W., Mitchell, C.A., 2005. The future for electrocoagulation as a localised water treatment technology. Chemosphere 59 (3), 355–367. doi:10.1016/j.chemosphere.2004.10.023.

Ito, A., Miura, J.I., Ishikawa, N., Umita, T., 2012. Biological oxidation of arsenite in synthetic groundwater using immobilised bacteria. Water Res. 46 (15), 4825–4831. doi:10.1016/j.watres.2012.06.013.

Jackman, T.A., Hughes, C.L., 2010. Formation of trihalomethanes in soil and groundwater by the release of sodium hypochlorite. Ground Water Monit. Remediat. 30 (1), 74–78. doi:10.1111/j.1745-6592.2009.01266.x.

Kamei-Ishikawa, N., Segawa, N., Yamazaki, D., Ito, A., Umita, T., 2017. Arsenic removal from arsenic-contaminated water by biological arsenite oxidation and chemical ferrous iron oxidation using a down-flow hanging sponge reactor. Water Sci. Technol. 17 (5), 1249–1259. doi:10.2166/ws.2017.025.

Kapaj, S., Peterson, H., Liber, K., Bhattacharya, P., 2006. Human health effects from chronic arsenic poisoning - A review. J. Environ. Sci. Health - Part A Toxic/Hazardous Substan. Environ. Eng. 41 (10), 2399–2428. doi:10.1080/10934520600873571.

Katsoyiannis, I.A., Zouboulis, A.I., 2004. Application of biological processes for the removal of arsenic from groundwaters. Water Res. 38 (1), 17–26. doi:10.1016/j.watres.2003.09.011.

Kim, M.J., Nriagu, J., 2000. Oxidation of arsenite in groundwater using ozone and oxygen. Sci. Total Environ. 247 (1), 71–79. doi:10.1016/S0048-9697(99)00470-2.

Kitahama, K., Kiriyama, R., Baba, Y., 1975. Refinement of the crystal structure of scorodite. Acta Crystallogr. Section B Struct. Crystallogr. Crystal Chem. 31 (1), 322–324. doi:10.1107/s056774087500266x.

Kobya, M., Demirbas, E., Ulu, F., 2016. Evaluation of operating parameters with respect to charge loading on the removal efficiency of arsenic from potable water by electrocoagulation. J. Environ. Chem. Eng. 4 (2), 1484–1494. doi:10.1016/j.jece.2016.02.016.

Kott, Y., Ribas, F., Frías, J., Lucena, F., 1997. Comparison between the evaluation of bacterial regrowth capability in a turbidimeter and biodegradable dissolved organic carbon bioreactor measurements in water. J. Appl. Microbiol. 83.

Kumar, P.R., Chaudhari, S., Khilar, K.C., Mahajan, S.P., 2004. Removal of arsenic from water by electrocoagulation. Chemosphere 55 (9), 1245–1252. doi:10.1016/j.chemosphere.2003.12.025.

Li, L., Van Genuchten, C.M., Addy, S.E.A., Yao, J., Gao, N., & Gadgil, A.J. (2012). *Modeling As(III) Oxidation and removal with Iron electrocoagulation in groundwater*. 10.1021/es302456b

Lytle, D.A., Chen, A.S., Sorg, T.J., Phillips, S., French, K., 2007. Microbial As(III) oxidation in water treatment plant filters. J. Am. Water Works Assoc. 99 (12), 72–86. doi:10.1002/j.1551-8833.2007.tb08108.x.

Magoč, T., Magoč, M., Salzberg, S.L., 2011. FLASH 27 (21), 2957–2963. doi:10.1093/bioinformatics/btr507.

McBeath, S.T., Mohseni, M., Wilkinson, D.P., 2020. Pilot-scale iron electrocoagulation treatment for natural organic matter removal. Environ. Technol. (United Kingdom) 41 (5), 577–585. doi:10.1080/09593330.2018.1505965.

Mollah, M.Y.A., Morkovsky, P., Gomes, J.A.G., Kesmez, M., Parga, J., Cocke, D.L., 2004. Fundamentals, present and future perspectives of electrocoagulation. J. Hazard. Mater. 114 (1–3), 199–210. doi:10.1016/j.jhazmat.2004.08.009.

Mondal, P., Bhowmick, S., Chatterjee, D., Figoli, A., Van der Bruggen, B., 2013. Remediation of inorganic arsenic in groundwater for safe water supply: a critical assessment of technological solutions. Chemosphere 92 (2), 157–170. doi:10.1016/j.chemosphere.2013.01.097, Pergamon.

Moussa, D.T., El-Naas, M.H., Nasser, M., Al-Marri, M.J., 2017. A comprehensive review of electrocoagulation for water treatment: potentials and challenges. J. Environ. Manage. 186, 24–41. doi:10.1016/j.jenvman.2016.10.032, Academic Press.

Muller, D., Lièvremont, D., Simeonova, D.D., Hubert, J.C., Lett, M.C., 2003. Arsenite oxidase aox genes from a metal-resistant β-proteobacterium. J. Bacteriol. 185 (1), 135–141. doi:10.1128/JB.185.1.135-141.2003.

Müller, S., Behrends, T., van Genuchten, C.M., 2019. Sustaining efficient production of aqueous iron during repeated operation of Fe(0)-electrocoagulation. Water Res. 155, 455–464. doi:10.1016/j.watres.2018.11.060.

Newville, M., 2001. IFEFFIT: interactive XAFS analysis and FEFF fitting. J. Synchrotron. Radiat. 8 (2), 322–324. doi:10.1107/S0909049500016964.

Nicomel, N.R., Leus, K., Folens, K., Van Der Voort, P., Du Laing, G., 2015. Technologies for arsenic removal from water: current status and future perspectives. Int. J. Environ. Res. Public Health 13 (1). doi:10.3390/ijerph13010062, ijerph13010062MDPI AG.

Podgorski, J., Berg, M., 2020. Global threat of arsenic in groundwater. Science 368 (6493), 845–850. doi:10.1126/science.aba1510.

Raven, K.P., Jain, A., Loeppert, R.H., 1998. Arsenite and arsenate adsorption on ferrihydrite: kinetics, equilibrium, and adsorption envelopes. Environ. Sci. Technol. 32 (3), 344–349. doi:10.1021/es970421p.

Redman, A.D., Macalady, D.L., Ahmann, D., 2002. Natural organic matter affects Arsenic speciation and sorption onto hematite. Environ. Sci. Technol. 36 (13), 2889–2896. doi:10.1021/es0112801.

Rehr, J.J., Albers, R.C., Zabinsky, S.I., 1992. High-order multiple-scattering calculations of x-ray-absorption fine structure. Phys. Rev. Lett. 69 (23), 3397–3400. doi:10.1103/PhysRevLett.69.3397.

Roberts, L.C., Hug, S.J., Ruettimann, T., Billah, M., Khan, A.W., Rahman, M.T., 2004. Arsenic removal with Iron(II) and Iron(III) in waters with high silicate and phosphate concentrations. Environ. Sci. Technol. 38 (1), 307–315. doi:10.1021/es0343205.

Roy, A., van Genuchten, C.M., Mookherjee, I., Debsarkar, A., Dutta, A., 2019. Concrete stabilization of arsenic-bearing iron sludge generated from an electrochemical arsenic remediation plant. J. Environ. Manage. 233, 141–150. doi:10.1016/j.jenvman.2018.11.062.

Santini, J.M., Sly, L.I., Schnagl, R.D., Macy, J.M., 2000. A new chemolithoautotrophic arsenite-oxidizing bacterium isolated from a gold mine: phylogenetic, physiological, and preliminary biochemical studies. Appl. Environ. Microbiol. 66 (1), 92–97. doi:10.1128/AEM.66.1.92-97.2000.

Schmidt, S.A., Gukelberger, E., Hermann, M., Fiedler, F., Großmann, B., Hoinkis, J., Ghosh, A., Chatterjee, D., Bundschuh, J., 2016. Pilot study on arsenic removal from groundwater using a small-scale reverse osmosis system—Towards sustainable drinking water production. J. Hazard. Mater. 318, 671–678. doi:10.1016/j.jhazmat.2016.06.005.

Sorlini, S., Gialdini, F., 2010. Conventional oxidation treatments for the removal of arsenic with chlorine dioxide, hypochlorite, potassium permanganate and monochloramine. Water Res. 44 (19), 5653–5659. doi:10.1016/j.watres.2010.06.032.

Sullivan, C., Tyrer, M., Cheeseman, C.R., Graham, N.J.D., 2010. Disposal of water treatment wastes containing arsenic - A review. Sci. Total Environ. 408 (8), 1770–1778. doi:10.1016/j.scitotenv.2010.01.010, Elsevier.

Sundman, A., 2014. Interactions Between Fe and Organic Matter and Their Impact On As(V) and P(V). Umeå Universitet, Doctoral dissertation http://umu.diva-portal.org/.

Thirunavukkarasu, O.S., Viraraghavan, T., Subramanian, K.S., 2003. Arsenic removal from drinking water using iron oxide-coated sand. Water Air Soil Pollut. 142 (1–4), 95–111. doi:10.1023/A:1022073721853, IssuesSpringer.

Toner, B.M., Santelli, C.M., Marcus, M.A., Wirth, R., Chan, C.S., McCollom, T., Bach, W., Edwards, K.J., 2009. Biogenic iron oxyhydroxide formation at mid-ocean ridge hydrothermal vents: juan de Fuca Ridge. Geochim. Cosmochim. Acta 73 (2), 388–403. doi:10.1016/j.gca.2008.09.035.

Tseng, W.P., 1977. Effects and dose response relationships of skin cancer and blackfoot disease with arsenic. Environ. Health Perspect. 19, 109–119. doi:10.1289/ehp.7719109.

van Genuchten, C.M., Addy, S.E.A., Peña, J., Gadgil, A.J., 2012. Removing arsenic from synthetic groundwater with iron electrocoagulation: an Fe and As K-edge EXAFS study. Environ. Sci. Technol. 46 (2), 986–994. doi:10.1021/es201913a.

van Genuchten, C.M., Peña, J., Amrose, S.E., Gadgil, A.J., 2014. Structure of Fe(III) precipitates generated by the electrolytic dissolution of Fe(0) in the presence of groundwater ions. Geochim. Cosmochim. Acta 127, 285–304. doi:10.1016/j.gca.2013.11.044.

Vandenabeele, J., de Beer, D., Germonpré, R., Verstraete, W., 1992. Manganese oxidation by microbial consortia from sand filters. Microb. Ecol. 24 (1), 91–108. doi:10.1007/BF00171973.

Vandermaesen, J., Lievens, B., Springael, D., 2017. Isolation and identification of culturable bacteria, capable of heterotrophic growth, from rapid sand filters of drinking water treatment plants. Res. Microbiol. 168 (6), 594–607. doi:10.1016/j.resmic.2017.03.008.

Wan, W., Pepping, T.J., Banerji, T., Chaudhari, S., Giammar, D.E., 2011. Effects of water chemistry on arsenic removal from drinking water by electrocoagulation. Water Res. 45 (1), 384–392. doi:10.1016/j.watres.2010.08.016.

Wang, Q., Garrity, G.M., Tiedje, J.M., Cole, J.R., 2007. Naïve Bayesian classifier for rapid assignment of rRNA sequences into the new bacterial taxonomy. Appl. Environ. Microbiol. 73 (16), 5261–5267. doi:10.1128/AEM.00062-07.

Waychunas, G.A., Rea, B.A., Fuller, C.C., Davis, J.A., 1993. Surface chemistry of ferrihydrite: part 1. EXAFS studies of the geometry of coprecipitated and adsorbed arsenate. Geochim. Cosmochim. Acta 57 (10), 2251–2269. doi:10.1016/0016-7037(93)90567-G.

Webb, S.M., 2005. SIXpack: a graphical user interface for XAS analysis using IFEFFIT. Physica Scripta T T115 (T115), 1011–1014. doi:10.1238/Physica.Topical.115a01011.

World Health Organization, 2004. Guidlines For Drinking-Water Quality, vol. 1. Recommendations, 3rd ed World Health Organization, Geneva, Switzerland.

Zhang, P., Tong, M., Yuan, S., Liao, P., 2014. Transformation and removal of arsenic in groundwater by sequential anodic oxidation and electrocoagulation. J. Contam. Hydrol. 164, 299–307. doi:10.1016/j.jconhyd.2014.06.009.